Prostaglandin $F_{2\alpha}$ Facilitates Hepatic Glucose Production Through CaMKIIγ/p38/FOXO1 Signaling Pathway in Fasting and Obesity

Yuanyang Wang,[1] Shuai Yan,[2] Bing Xiao,[2,3] Shengkai Zuo,[2] Qianqian Zhang,[2] Guilin Chen,[1] Yu Yu,[2,4] Di Chen,[2,5] Qian Liu,[1] Yi Liu,[2] Yujun Shen,[1] and Ying Yu[1,2]

Diabetes 2018;67:1748–1760 | https://doi.org/10.2337/db17-1521

Gluconeogenesis is drastically increased in patients with type 2 diabetes and accounts for increased fasting plasma glucose concentrations. Circulating levels of prostaglandin (PG) $F_{2\alpha}$ are also markedly elevated in diabetes; however, whether and how $PGF_{2\alpha}$ regulates hepatic glucose metabolism remain unknown. Here, we demonstrated that $PGF_{2\alpha}$ receptor (F-prostanoid receptor [FP]) was upregulated in the livers of mice upon fasting- and diabetic stress. Hepatic deletion of the FP receptor suppressed fasting-induced hepatic gluconeogenesis, whereas FP overexpression enhanced hepatic gluconeogenesis in mice. FP activation promoted the expression of gluconeogenic enzymes (PEPCK and glucose-6-phosphatase) in hepatocytes in a FOXO1-dependent manner. Additionally, FP coupled with G_q in hepatocytes to elicit Ca^{2+} release, which activated Ca^{2+}/calmodulin-activated protein kinase IIγ (CaMKIIγ) to increase FOXO1 phosphorylation and subsequently accelerate its nuclear translocation. Blockage of p38 disrupted CaMKIIγ-induced FOXO1 nuclear translocation and abrogated FP-mediated hepatic gluconeogenesis in mice. Moreover, knockdown of hepatic FP receptor improved insulin sensitivity and glucose homeostasis in *ob/ob* mice. FP-mediated hepatic gluconeogenesis via the CaMKIIγ/p38/FOXO1 signaling pathway, indicating that the FP receptor might be a promising therapeutic target for type 2 diabetes.

Type 2 diabetes constitutes a major worldwide public health burden and is expected to affect >642 million adults by 2040 (1). Type 2 diabetes is characterized by hyperglycemia, insulin resistance, and β-cell dysfunction, and often is associated with low-grade chronic inflammation (2). Blood glucose homeostasis is maintained by the balance between hepatic glucose production (HGP) (glycogenolysis and gluconeogenesis) and glucose utilization by peripheral tissues. In patients with type 2 diabetes, hepatic gluconeogenesis is considerably elevated and contributes to both fasting and postprandial hyperglycemia, and suppressing hepatic gluconeogenesis improves insulin sensitivity and glucose homeostasis, making it an attractive target for the treatment of diabetes (3). Hepatic gluconeogenesis is tightly controlled by rate-limiting gluconeogenic enzymes, including PEPCK (PCK1), glucose-6-phosphatase (G6Pase), and fructose-1,6-bisphosphatase. The quantity and activity of these essential enzymes are mainly regulated by the pancreatic hormones insulin and glucagon (4). In addition to hormonal control, hepatic gluconeogenesis is also directly regulated by inflammatory mediators, such as cytokines (5) and phospholipid derivatives (6,7).

Prostaglandin (PG) $F_{2\alpha}$ is a bioactive lipid metabolite of arachidonic acid produced through the sequential reaction of cyclooxygenases and PGF synthase. $PGF_{2\alpha}$ exerts a wild range of pathological and physiological functions, including

[1]Department of Pharmacology, School of Basic Medical Sciences, 2011 Collaborative Innovation Center of Tianjin for Medical Epigenetics, Key Laboratory of Immune Microenvironment and Disease (Ministry of Education), Tianjin Medical University, Tianjin, People's Republic of China

[2]Key Laboratory of Food Safety Research, Institute for Nutritional Sciences, Shanghai Institutes for Biological Sciences, Graduate School of the Chinese Academy of Sciences, Chinese Academy of Sciences, Shanghai, People's Republic of China

[3]State Key Laboratory for Medical Genomics, School of Life Science and Biotechnology, Shanghai Jiao Tong University, Shanghai, People's Republic of China

[4]Department of Pediatric Cardiology, Xinhua Hospital affiliated to Shanghai Jiao Tong University School of Medicine, Shanghai, People's Republic of China

[5]Department of Microbiology and Immunology, University of Michigan Medical School, Ann Arbor, MI

Corresponding author: Ying Yu, yuying@sibs.ac.cn or yuying@tmu.edu.cn, or Yujun Shen, yujun_shen@tmu.edu.cn.

Received 14 December 2017 and accepted 1 May 2018.

This article contains Supplementary Data online at http://diabetes.diabetesjournals.org/lookup/suppl/doi:10.2337/db17-1521/-/DC1.

See accompanying article, p. 1742.

reproduction (8), blood pressure (9), and bone remodeling (10), by binding to its receptor (F-prostanoid [FP]). Experimental and clinical studies showed that $PGF_{2\alpha}$ is involved in different inflammatory conditions, including rheumatic diseases, asthma, atherosclerosis, ischemia-reperfusion, septic shock, and obesity (11). Interestingly, increased $PGF_{2\alpha}$ metabolite production is found in urine from patients with both type 1 diabetes (12) and type 2 diabetes (13), and plasma $PGF_{2\alpha}$ levels can be used as a marker to predict glycemic control and oxidation status (14). Moreover, hepatic $PGF_{2\alpha}$ production is also significantly increased in fasted, high-fat diet (HFD)–fed, or diabetic animals (7). FP receptor is expressed in hepatocytes (15); however, whether an activated $PGF_{2\alpha}$/FP axis is implicated in aberrant glucose metabolism in diabetes remains largely unclear.

In this study, we demonstrated that the activation of FP receptor increased fasting-induced hepatic gluconeogenesis in mice by upregulating gluconeogenic genes (PCK1 and G6Pase) in a FOXO1-dependent manner. FP activation promoted FOXO1 nuclear translocation by stimulating G_q-mediated Ca^{2+}/calmodulin-activated protein kinase IIγ (CaMKIIγ) signaling, with p38 required for FP/CaMKIIγ-mediated FOXO1 nuclear translocation. Moreover, the silencing of hepatic FP receptor–ameliorated glucose metabolism in obese mice. Therefore, FP activation facilitated hepatic gluconeogenesis through the CaMKIIγ/p38/FOXO1 signaling pathway under both fasting and diabetic conditions.

RESEARCH DESIGN AND METHODS

Mouse Models

Human FP (hFP) hepatocyte transgenic (HCTG) and nontransgenic (NTG) littermates were obtained from the mating of Tg-hFP-$STOP^{Flox}$ (16) and Alb^{Cre} mice. FP exon2-floxed mice ($FP^{F/F}$) were generated through CRISPR/Cas9 technology by Shanghai Biomodel Organism Science & Technology Development Co., Ltd. (Shanghai, People's Republic of China) and crossed with Alb^{Cre} mice to obtain hepatic FP-deficient mice ($FP^{F/F}Alb^{cre}$). All mice used were from a C57BL/6 background. For inhibitor treatment, 8-week-old HCTG and NTG mice were intraperitoneally injected with KN-93 (3 mg/kg) (MedChem Express, Monmouth Junction, NJ) three times weekly for 1 week (17) or with SB202190 (2.5 μmol/L/kg) (Sigma-Aldrich, St. Louis, MO) daily for 1 week (18). All animals were maintained and used in accordance with the guidelines of the Institutional Animal Care and Use Committee of the Institution for Nutritional Sciences, Shanghai Institutes for Biological Sciences, Chinese Academy of Sciences, People's Republic of China.

Genotyping and Quantitative Real-time PCR

DNA was extracted from mice tails using the proteinase-K-chloroform method, and PCR was performed on an S1000 thermal cycler (Bio-Rad, Hercules, CA). RNA was isolated from tissues or cultured cells using TRIzol (Invitrogen, Carlsbad, CA) and reverse transcribed to cDNA using an RT Reagent Kit (TaKaRa, Dalian, People's Republic of China). The resulting cDNA was amplified for 40 cycles on a C1000 Thermal Cycler (Bio-Rad) using SYBR Green PCR mix (TaKaRa). Values were normalized to actin mRNA or 18S rRNA. See Supplementary Tables 1 and 2 for primer sequences.

Immunofluorescence

The frozen sections from liver or chamber slides with hepatocytes were washed with PBS and fixed in cold acetone. To block nonspecific binding of antibodies, samples were incubated with PBS containing 3% BSA and 0.1% Triton X-100 (for permeabilization) for 30 min. The samples were then incubated with mCherry fluorescent protein (1:200; Abbkine, Redlands, CA) or FOXO1 (1:500; Cell Signaling Technology, Danvers, MA) overnight at 4°C. Slides were then washed with PBS three times and incubated with secondary antibodies conjugated with Alexa Fluor 594 or Alexa Fluor 633 (Invitrogen) for 1 h at room temperature. ProLong Gold Antifade Reagent with DAPI (Invitrogen) was applied to mount and counterstain the slides. Images were obtained using confocal microscopy (IX51; Olympus, Center Valley, PA).

Western Blot

Total protein and cytosolic and nuclear protein fractions were isolated from tissues or cultured cells using a protein extraction kit (Beyotime, Shanghai, People's Republic of China), followed by separation by SDS-PAGE, transfer to nitrocellulose membranes, and probing with different primary antibodies against PCK1, p38, and lamin B (Proteintech, Wuhan, People's Republic of China); G6Pase and CaMKIIγ (Santa Cruz Biotechnology, Dallas, TX); α-tubulin, phospho-Thr287 CaMKIIγ, phospho-p38, FOXO1, and hemagglutinin (HA)-Tag (Cell Signaling Technology); hFP (Epitomics, Burlingame, CA); and β-actin (Sigma-Aldrich). The membranes were then conjugated with a horseradish peroxidase–labeled secondary antibody in blocking buffer for 2 h at room temperature. Blots were developed using enhanced chemiluminescence reagents (Pierce, Rockford, IL), followed by densitometric quantification using ImageJ (National Institutes of Health, Bethesda, MD). See Supplementary Table 3 for antibodies.

Live Imaging

Male mice (8 weeks old) were injected with G6P-Luc adenoviruses (1×10^8 plaque-forming units) by tail vein. On day 5 after adenovirus delivery, mice were subjected to fasting for 8 h before imaging, followed by intraperitoneal injection with 100 mg/kg sterile firefly D-luciferin (Biosynth, Itasca, IL). After 10 min, mice were imaged on the IVIS 100 Imaging System, and images were analyzed with Living Image software (Xenogen, Alameda, CA).

Adenovirus Construction

Adenoviruses were constructed using the AdEasy Adenoviral System (Qibogene, Irvine, CA) as previously described (19). For short hairpin RNA (shRNA) adenovirus, synthetic hFP, p38, and CaMKIIγ shRNA was inserted into the pGE1 plasmid under the control of U6 promoter, then a fragment containing shRNA and U6 promoter was digested

and cloned into the pAd-Track-cytomegalovirus (CMV) construct [pAd-Track-CMV] containing CMV-green fluorescent protein cassette. The empty vector [pAd-Track-CMV] was used as a control. For dominant-negative (DN)-FOXO1 adenovirus, DN-FOXO1 cDNA was inserted into the pAd-Track-CMV(+) construct under the control of the CMV promoter. The empty vector [pAd-Track-CMV(+)] was used as a DN-FOXO1 cDNA control. For WT-Flag-FOXO1and 9A-Flag-FOXO1 expressing adenovirus (20), cDNAs were first inserted into a pAd-Track-CMV(+) plasmid using CMV promoter, and then the constructs were subcloned into the pAd-Easy-1 adenoviral-backbone vector through homologous recombination in BJ5183. Adenoviral DNA was linearized by *Pac*I restriction digestion and transfected into HEK293 cells using Lipofectamine 2000 (Invitrogen) for adenovirus packaging. After several rounds of propagation, recombinant adenovirus was purified by ultracentrifugation (Beckman, Urbana, IL) in a cesium chloride gradient. See Supplementary Table 4 for shRNA sequences.

Metabolic Assessments

Insulin tolerance tests were performed by intraperitoneal injection of 0.8 units/kg insulin after 6 h of fasting, and pyruvate tolerance tests (PTTs) were performed by intraperitoneal injection of 2 g/kg sodium pyruvate after overnight fasting. Fasting blood glucose was measured by obtaining a tail-blood sample after 12 h of fasting. Serum triglyceride (TG) and total cholesterol, as well as liver glycogen levels, were measured using assay kits (BJKT, Beijing, People's Republic of China).

Cell Culture and Treatments

Primary mouse hepatocytes were isolated from 8- to 12-week-old mice using a two-step collagenase-perfusion technique as described previously (21). Hepatocytes were cultured in DMEM supplemented with 25 mmol/L glucose, 10% FBS, and 50 μg/mL penicillin and streptomycin at 37°C and 5% CO_2/95% air. Glucagon (100 nmol/L) and $PGF_{2\alpha}$ (100 nmol/L) from Cayman Chemical Company (Ann Arbor, MI), and pertussis toxin (PTX), Wortmannin, U73122, KN-93, and SB202190 from Sigma-Aldrich were used to treat hepatocytes, as indicated.

Primary HGP

Primary hepatocyte glucose production was measured as previously described (7,22). Briefly, isolated hepatocytes were cultured in monolayer in glucose- and phenol-free DMEM with 20 mmol/L sodium lactate and 1 mmol/L sodium pyruvate for 6 h after overnight FBS starvation, and glucose levels were measured using a glucose assay kit (Sigma-Aldrich). Total protein in the cell lysate was used for normalization. For adenovirus experiments, a hepatocyte glucose production test was performed 48 h after adenovirus infection.

Intracellular Measurement of Free Ca^{2+}

Ca^{2+} transients were recorded using a laser-scanning confocal microscope (Carl Zeiss, Oberkochen, Germany) as previously described (23). Briefly, hepatocytes seeded on chamber slides (Thermo Fisher Scientific, Waltham, MA) were loaded with 5 μmol/L Fluo 3-AM (Dojindo Laboratories, Kumamoto, Japan) for 30 min, washed, and imaged under an IX71 Fluorescence Microscope (Olympus). Fluo-3 was excited at 488 nm.

Statistical Analysis

Results are represented as the mean ± SEM. All statistical analyses were subjected to Student *t* test or two-way ANOVA, followed by the Bonferroni post hoc test using GraphPad Prism 5 software (GraphPad, La Jolla, CA). A P value of <0.05 was considered statistically significant.

RESULTS

The Hepatic $PGF_{2\alpha}$/FP Axis Promotes Gluconeogenesis in Mice in Response to Fasting

$PGF_{2\alpha}$ production in the liver is markedly elevated in mice in response to fasting and HFD treatment or those with obesity (7), conditions associated with augmented hepatic gluconeogenesis. Accordingly, we observed significantly upregulated FP expression in livers from fasted, *ob*/*ob*, and HFD-treated mice (Fig. 1*A*), indicating that the $PGF_{2\alpha}$/FP axis was activated in the liver upon fasting and diabetic stress. Interestingly, hepatic knockdown of FP receptor by intravenous delivery of shRNA adenovirus (Ad-FP-shRNA) (Fig. 1*B* and *C*) markedly reduced circulating glucose concentrations after an 8- to 12-h fast (Fig. 1*D*) and attenuated gluconeogenic capacity in mice after pyruvate infusion (Fig. 1*E*), but did not affect hepatic glycogen content under fasting conditions (Supplementary Fig. 1). Consistently, FP knockdown led to significant decreases in the expression of hepatic gluconeogenic genes, such as PCK1 and G6Pase, without altering the expression of the hepatic glycogenolysis gene glycogen phosphorylase (*Pygl*) under fasting conditions in mice (Fig. 1*F*–*H*). Similarly, in isolated primary hepatocytes, FP knockdown significantly reduced glucose output after pyruvate challenge (Fig. 1*I*) and suppressed gluconeogenic gene expression (*G6pase* and *Pck1*) without affecting glycogenolytic gene expression (*Pygl*) (Fig. 1*J*–*L*). Furthermore, FP knockdown improved insulin sensitivity in mice (Fig. 1*M*). These results suggested that FP is directly involved in hepatic gluconeogenesis by promoting hepatic gluconeogenic gene expression under both physiological and pathological conditions.

To examine whether FP overexpression in hepatocytes influences gluconeogenesis in vivo, we generated hFP transgenic mice using a Cre-loxp strategy. Two strains exhibiting hepatic hFP overexpression (HCTG-A and HCTG-E) were obtained, with NTG littermates serving as controls (Supplementary Fig. 2*A* and *B*). In HCTG mice, the hFP gene was expressed under the control of the albumin promoter in hepatocytes by Cre-mediated mCherry sequence excision (Supplementary Fig. 2*C*), leading to highly effective and selective expression in livers (Supplementary Fig. 2*D* and *E*). There were no differences in body weight, body composition, and plasma TG and cholesterol levels between wild-type and HCTG mice (Supplementary Fig. 3*A*–*C*). Notably,

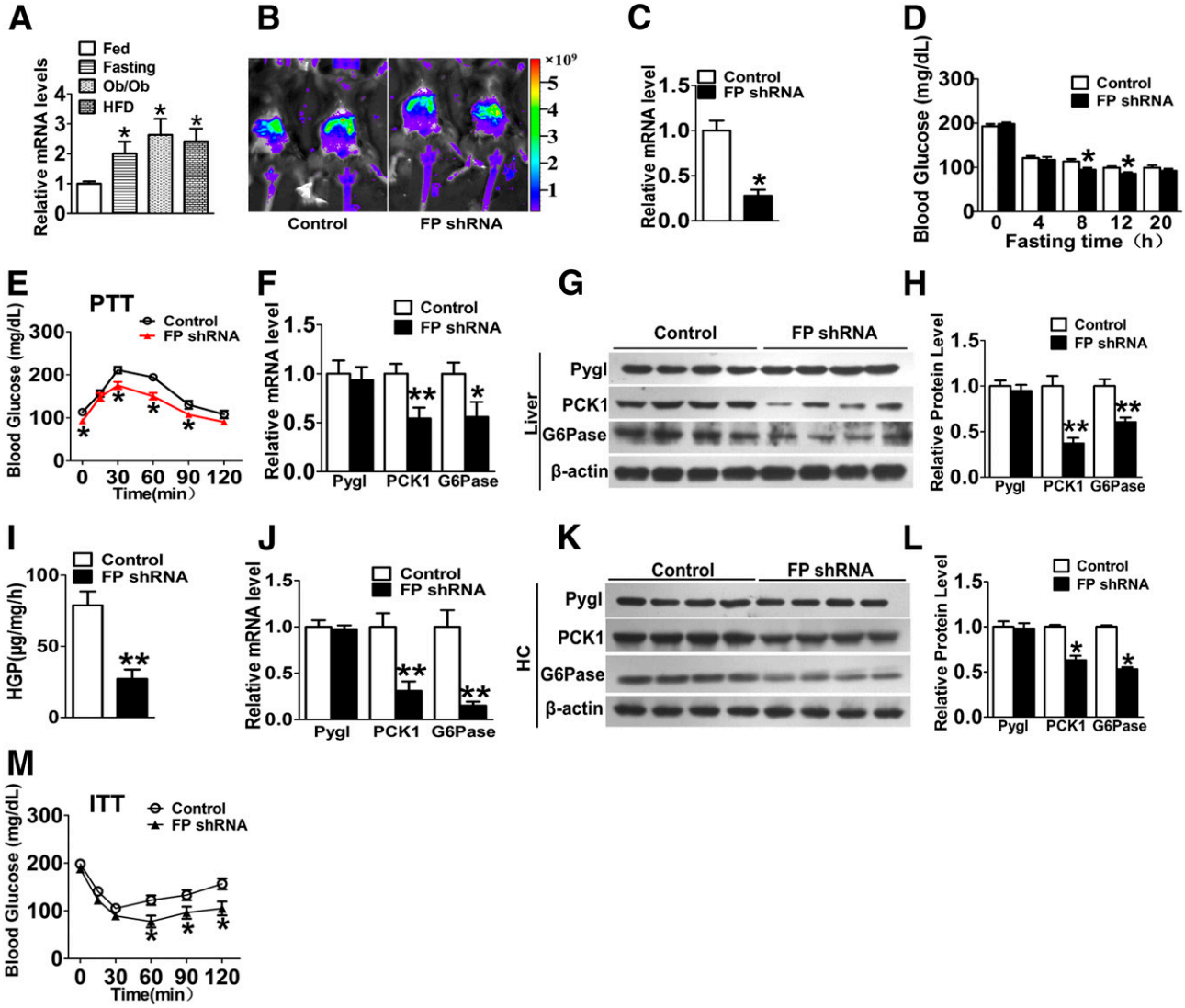

Figure 1—Knockdown of FP receptor in livers suppresses hepatic glucose output in mice. *A*: mRNA expression levels of FP in livers from mice fed a diet of regular chow (Fed), HFD, those fasted, and those that were *ob/ob*. $^{*}P < 0.05$ vs. Fed ($n = 4$). *B*: Representative live images of green fluorescent protein fluorescence intensity in mouse liver at day 7 after tail infusion of FP shRNA or control adenovirus (Vector). *C*: FP mRNA expression levels in livers at day 7 after tail infusion of FP shRNA or control adenovirus. $^{*}P < 0.05$ vs. Control ($n = 8$). *D*: Blood glucose alterations in response to fasting in mice after FP shRNA or control adenovirus infusion. $^{*}P < 0.05$ vs. Control ($n = 10$). *E*: PTT (2.0 g/kg pyruvate i.p.) in mice after FP shRNA or control adenovirus infusion. $^{*}P < 0.05$ vs. Control ($n = 10$). *F*: Hepatic mRNA levels of *Pygl*, *Pck1*, and *G6pase* in mice after 8 h of fasting and FP shRNA or control adenovirus infusion. $^{*}P < 0.05$; $^{**}P < 0.01$ vs. Control ($n = 8$). *G*: Immunoblotting assay of hepatic PYGL, PCK1, and G6Pase in mice fasted for 8 h after FP shRNA or control adenovirus infusion. *H*: Quantification of PYGL, PCK1, and G6Pase expression in *G*. $^{**}P < 0.01$ vs. Control ($n = 4$). *I*: Glucose production in primary hepatocytes after FP shRNA or control adenovirus infection. $^{**}P < 0.01$ vs. Control ($n = 6$). *J*: mRNA levels of *Pygl*, *Pck1*, and *G6pase* in primary hepatocytes after FP shRNA or adenovirus infection. $^{**}P < 0.01$ vs. Control ($n = 6$). *K*: Immunoblotting assay for PYGL, PCK1, and G6Pase in primary hepatocytes (HC) after FP shRNA or control adenovirus infection. *L*: Quantification of PYGL, PCK1, and G6Pase expression in *K*. $^{*}P < 0.05$ vs. Control ($n = 4$). *M*: Insulin tolerance test (ITT) in mice after FP shRNA or control adenovirus infection. $^{*}P < 0.05$ vs. Control ($n = 10$).

HCTG mice showed significantly higher blood glucose concentrations after 8–12 h of fasting compared with NTG mice (Fig. 2*A*) and exhibited enhanced HGP according to PTT results (Fig. 2*B*) along with upregulated hepatic gluconeogenic gene expression (*G6pase* and *Pck1*) (Fig. 2*C*–*G*). Importantly, hFP transgenic mice also showed less sensitivity to insulin challenge (Fig. 2*H*). We also examined hepatic transcription activity of gluconeogenic genes in HCTG mice by infusion of the adenoviral G6Pase-luciferase (Ad-G6Pase-Luc) reporter containing both FOXO1-binding and cAMP-responsive element–binding sites that mediate upregulation of gluconeogenic genes during fasting (24). During fasting, Ad-G6Pase-Luc activity was markedly elevated in HCTG mice compared with control mice (Fig. 2*I* and J). Moreover, forced expression of the hFP gene increased basal HGP in culture, and $PGF_{2\alpha}$ treatment further augmented HGP in HCTG hepatocytes (Fig. 3*A*). Furthermore, $PGF_{2\alpha}$ induced gluconeogenic gene expression (*G6pase* and *Pck1*) at both the

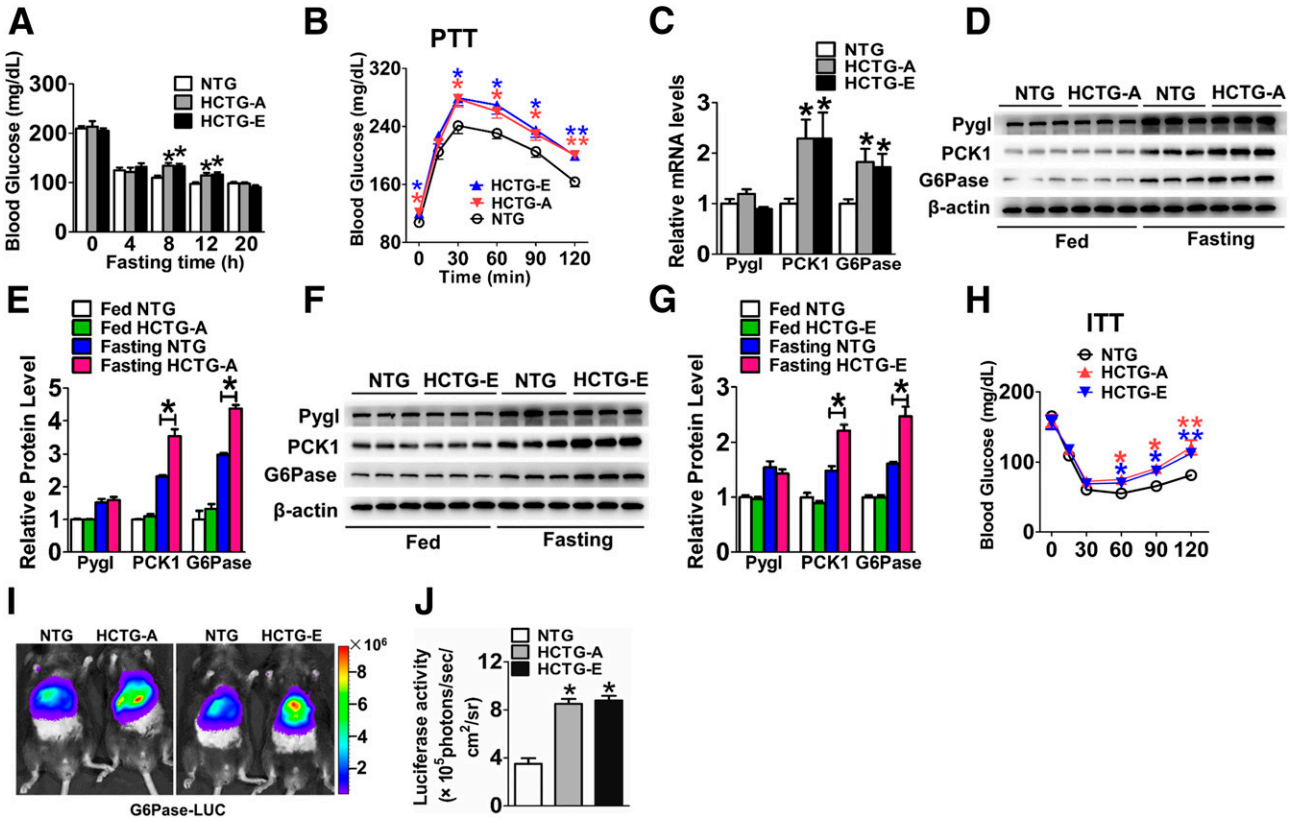

Figure 2—Hepatic overexpression of hFP promotes hepatic glucose output in transgenic mice. *A*: Blood glucose levels in response to fasting in mice. *$P < 0.05$ vs. NTG ($n = 9$). *B*: PTT (2.0 g/kg pyruvate i.p.) in HCTG mice. *$P < 0.05$; **$P < 0.01$ vs. NTG ($n = 9$). *C*: Hepatic mRNA levels of *Pygl*, *Pck1*, and *G6pase* in mice fasted for 8 h. *$P < 0.05$ vs. NTG ($n = 8$). *D*: Immunoblotting assays for hepatic PYGL, PCK1, and G6Pase in HCTG-A mice after feeding or 8 h of fasting. *E*: Quantification of PYGL, PCK1, and G6Pase expression in *D*. *$P < 0.05$ vs. as indicated ($n = 5$). *F*: Immunoblotting assays for hepatic PYGL, PCK1, and G6Pase in HCTG-E mice after feeding or 8 h of fasting. *G*: Quantification of PYGL, PCK1, and G6Pase expression in *F*. *$P < 0.05$ vs. as indicated ($n = 5$). *H*: Insulin tolerance test (ITT) in HCTG and NTG littermates. *$P < 0.05$; **$P < 0.01$ vs. NTG ($n = 8$). *I*: Representative live images of hepatic G6Pase-Luc activity in mice fasted for 8 h after adenovirus injection for 5 days. *J*: Quantification of luciferase activity in *I*. *$P < 0.05$ vs. NTG ($n = 6$).

mRNA and protein levels in NTG and HCTG hepatocytes without altering glycogenolytic gene (*Pygl*) expression (Fig. 3*B–E*). Consistently, Ad-G6Pase-Luc activity was markedly increased in response to $PGF_{2\alpha}$ in cultured HCTG hepatocytes compared with levels observed in NTG cells (Fig. 3*F*). Therefore, these results indicated that $PGF_{2\alpha}$/FP promoted hepatic gluconeogenesis by upregulating gluconeogenic genes.

FP Mediates Hepatic Gluconeogenesis by Activating Ca^{2+}/CaMKIIγ Signaling

The FP receptor might couple to different G-proteins to trigger downstream-signaling molecules, such as G_q to mobilize cytosolic Ca^{2+} or G_i to reduce intracellular cAMP levels (25). To determine which G-protein signal is involved in FP-mediated gluconeogenesis, primary hepatocytes were treated with the phospholipase C inhibitor U73122 (inhibits Ca^{2+} release), the G_i inhibitor pertussis toxin, or the phosphoinositide 3-kinase inhibitor Wortmannin in the presence of $PGF_{2\alpha}$, followed by the monitoring of glucose production after pyruvate challenge. U73122 significantly suppressed $PGF_{2\alpha}$-induced glucose output and gluconeogenic gene expression (*G6pase* and *Pck1*) in HCTG hepatocytes (Fig. 4*A* and *B*). Additionally, hFP overexpression resulted in significantly elevated intercellular Ca^{2+} concentrations in hepatocytes, which was blocked by U73122 treatment (Fig. 4*C*). Because the Ca^{2+}-sensing kinase CaMKII is essential for gluconeogenesis in fasting conditions and obesity (26), we then examined the expression levels of CaMKII isoforms (α, β, γ, and δ) in mouse hepatocytes, finding only abundant expression of CaMKIIγ (Fig. 4*D* and *E*). FP knockdown significantly suppressed CaMKIIγ phosphorylation in cultured hepatocytes and livers in mice (Fig. 4*F–I*), whereas hFP overexpression dramatically increased CaMKIIγ phosphorylation in cultured hepatocytes and livers from HCTG mice (Fig. 4*J–L*). Blockage of Ca^{2+} influx by U-73122 effectively attenuated increased CaMKIIγ phosphorylation levels in hFP-overexpressing hepatocytes from HCTG mice (Fig. 4*M*). Furthermore, treatment with the specific CaMKII inhibitor KN-93 suppressed CaMKIIγ phosphorylation, diminished the increased HGP in hFP-overexpressing hepatocytes in response to pyruvate

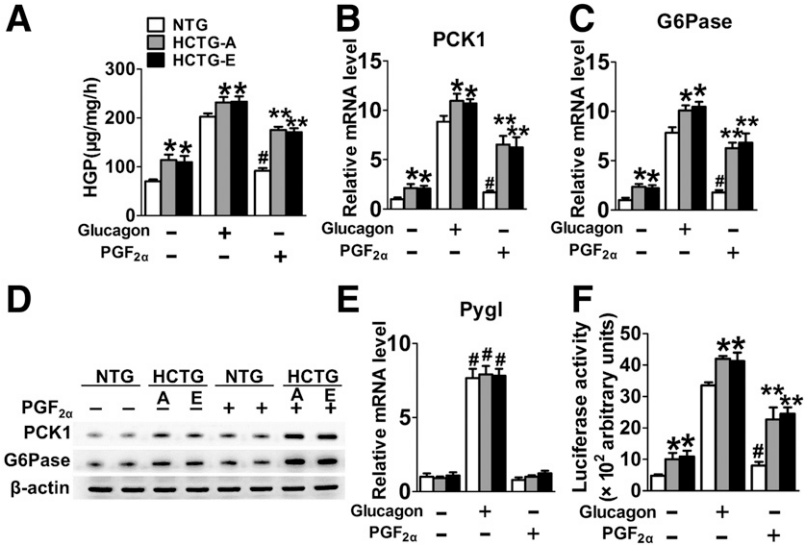

Figure 3—Overexpression of hFP receptor promotes glucose production in primary hepatocytes. *A*: Glucose production in primary hepatocytes isolated from NTG and HCTG mice in response to glucagon (100 nmol/L), $PGF_{2\alpha}$ (100 nmol/L), or vehicle control. $^*P <$ 0.05; $^{**}P < 0.01$ vs. NTG, $\#P < 0.05$ vs. vehicle ($n = 6$). *B–D*: Expression of PCK1 and G6Pase in primary hepatocytes in response to glucagon, $PGF_{2\alpha}$, or vehicle control. $^*P < 0.05$; $^{**}P < 0.01$ vs. NTG, $\#P < 0.05$ vs. vehicle ($n = 6$). *E*: mRNA expression levels of *Pygl* in primary hepatocytes in response to glucagon, $PGF_{2\alpha}$, or vehicle control. *F*: G6Pase-Luc activity assay in primary hepatocytes. $^*P < 0.05$; $^{**}P < 0.01$ vs. NTG, $\#P < 0.05$ vs. vehicle ($n = 6$).

challenge (Fig. 4*N*), and blunted the upregulated gluconeogenic protein expression in hepatocytes from HCTG mice (Fig. 4*O*). Consistent with in vitro observations, KN-93 treatment also abrogated elevated blood glucose concentrations in HCTG mice observed after 8–12 h of fasting (Fig. 4*P*). Collectively, these results showed that CaMKIIγ mediated $PGF_{2\alpha}$-induced hepatic gluconeogenesis in mice upon fasting.

CaMKIIγ Facilitates $PGF_{2\alpha}$-Induced Hepatic Gluconeogenesis Through p38

CaMKII modulates glucose metabolism and hepatic insulin signaling through its downstream mediator p38 mitogen-activated protein kinase (26,27), and p38 is involved in fasting-induced gluconeogenesis (27,28). Strikingly, FP knockdown significantly inhibited p38 phosphorylation, which represents the activated form of p38, in primary hepatocytes (Fig. 5*A*). By contrast, hFP overexpression enhanced p38 phosphorylation in primary hepatocytes in either the presence or absence of exogenous $PGF_{2\alpha}$ stimulation (Fig. 5*B*). Additionally, the inhibition of intracellular Ca^{2+} influx by U-73122 or CaMKII activity by KN-93 abrogated induction of p38 phosphorylation in HCTG hepatocytes (Fig. 5*C* and *D*). In agreement with the in vitro observations, phosphorylated p38 levels in mouse livers were reduced by Ad-FP-shRNA infection (Fig. 5*E* and *F*), whereas they were elevated by hepatic overexpression of hFP receptor (Fig. 5*G*). Importantly, the administration of SB202190, which suppresses p38 activity according to reductions in phosphorylated mitogen-activated protein kinase–activated protein kinase 2 (p-MK2; a p38 kinase target), attenuated upregulated gluconeogenic protein expression (*G6pase* and *Pck1*) in HCTG hepatocytes (Fig. 5*H*), thereby blunting increased HGP in HCTG hepatocytes (Fig. 5*I*). Consistently, SB202190 treatment also eliminated elevations in plasma glucose concentrations in HCTG mice after fasting for 8–12 h (Fig. 5*J*). Moreover, silencing of CaMKIIγ, or p38α, a dominant expressed isoform in liver (28), significantly attenuated the glucose production and suppressed the upregulation of gluconeogenic gene expression (G6pase and Pck1) in HCTG hepatocytes, respectively (Supplementary Fig. 4*A–F*). Therefore, $PGF_{2\alpha}$ promoted hepatic gluconeogenesis by activating CaMKIIγ/p38 signaling.

FP Activation Promotes Nuclear Translocation of FOXO1 Through the CaMKIIγ/p38 Signaling Pathway

FOXO1 is a major transcription factor involved in glucose metabolism and is regulated mainly through changes in its cellular localization between the cytoplasm and nucleus (29). p38 can directly phosphorylate FOXO1 at five different sites (20), thereby promoting FOXO1 nuclear translocation and facilitating HGP in hepatocytes (26). We hypothesized that FP might facilitate HGP through P38-mediated FOXO1 nuclear localization. Interestingly, FP knockdown led to relative cytoplasmic accumulation of FOXO1 (Fig. 6*A* and *B*), whereas hFP overexpression markedly increased nuclear translocation of FOXO1 in both cultured hepatocytes and livers in mice (Fig. 6*C–E*). Of note, either knockdown or overexpression of FP did not affect the total FOXO1 protein level in mouse hepatocytes and liver tissues (Fig. 6*A–D*). Inhibition of FOXO1 by adenoviral delivery of HA-tagged DN-FOXO1, a truncated mutant of FOXO1 containing the entire DNA-binding domain but lacking the transactivation domain (30), abrogated the elevated expression of *G6pase* and *Pck1* in HCTG hepatocytes and suppressed the

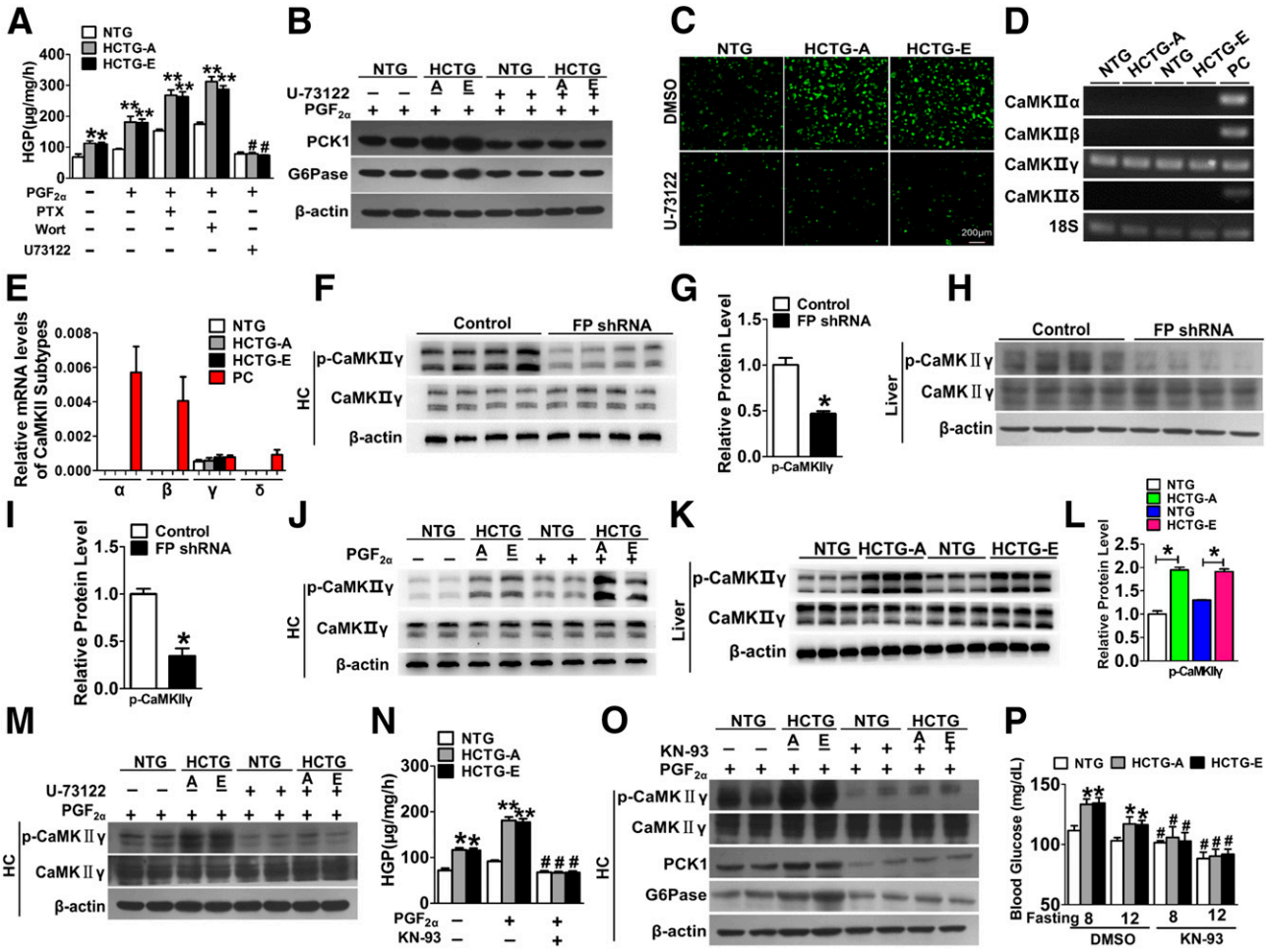

Figure 4—FP mediates hepatic gluconeogenesis by activating Ca^{2+}/CaMKIIγ signaling. *A*: Glucose production in NTG and HCTG hepatocytes treated with PTX, Wortmannin, or U73122, respectively, in the presence of $PGF_{2\alpha}$. PTX, G_i-protein inhibitor; Wort, Wortmannin, phosphoinositide 3-kinase inhibitor; U73122, phospholipase C inhibitor. $^*P < 0.05$ vs. NTG, $^{**}P < 0.01$ vs. NTG, $\#P < 0.05$ vs. with $PGF_{2\alpha}$ (n = 5). *B*: Immunoblotting analysis of PCK1 and G6Pase proteins in primary hepatocytes treated with PTX, Wortmannin, or U73122 in the presence of $PGF_{2\alpha}$. *C*: Detection of intracellular Ca^{2+} in NTG and HCTG hepatocytes. Scale bar, 200 μm. *D*: Expression levels of CaMKII isoforms (α, β, γ, and δ) in NTG and HCTG hepatocytes. PC, positive control (brain tissues). *E*: mRNA expression levels of CaMKII isoforms in HCTG and NTG hepatocytes. *F*: Immunoblotting analysis of phospho-CaMKIIγ (p-CaMKIIγ) in primary hepatocytes (HC) after FP shRNA adenovirus infection. *G*: Quantification of p-CaMKIIγ expression in *F*. $^*P < 0.05$ vs. Control (n = 4). *H*: Immunoblotting analysis of hepatic p-CaMKIIγ in mice fasted for 8 h after infection with FP shRNA or control adenovirus. *I*: Quantification of p-CaMKIIγ and total CaMKIIγ expression in *H*. $^*P < 0.05$ vs. Control (n = 4). *J*: Immunoblotting analysis of phospho-CaMKIIγ in cultured NTG and HCTG hepatocytes. *K*: Immunoblotting analysis of phospho-CaMKIIγ in livers from NTG and HCTG mice fasted for 8 h. *L*: Quantification of p-CaMKIIγ and total CaMKIIγ expression in *K*. $^*P < 0.05$ vs. as indicated (n = 4). *M*: Immunoblotting analysis of p-CaMKIIγ in cultured NTG and HCTG hepatocytes in the presence of absence of U73122 treatment. *N*: Glucose production in NTG and HCTG hepatocytes in response to $PGF_{2\alpha}$ in the presence or absence of KN-93 treatment. KN-93, CaMKII inhibitor. $^*P < 0.05$; $^{**}P < 0.01$ vs. NTG, $\#P < 0.05$ vs. with $PGF_{2\alpha}$ (n = 5). *O*: Immunoblotting analysis of PCK1, G6Pase, and p-CaMKIIγ proteins in NTG and HCTG hepatocytes in response to $PGF_{2\alpha}$ and in the presence or absence of KN-93 treatment. *P*: Plasma blood glucose levels in NTG and HCTG mice after 8 and 12 h fasting in the presence of absence of KN-93 treatment. $^*P < 0.05$; $\#P < 0.05$ vs. DMSO (n = 8).

induction of $PGF_{2\alpha}$-induced HGP in HCTG hepatocytes after pyruvate challenge (Fig. 6*F* and *G*). In vivo transfection of the DN-FOXO1 adenovirus also completely eliminated elevated plasma glucose concentrations in HCTG mice after an 8- to 12-h fast (Fig. 6*H*). Furthermore, the blockade of intracellular Ca^{2+} flux (via CaMKII) or p38 activity impeded nuclear accumulation of FOXO1 in HCTG hepatocytes in response to $PGF_{2\alpha}$ (Fig. 6*I* and *K*). Finally, mutation of p38 phosphorylation sites in FOXO1 protein (20) led to a nuclear translocation defect in response to $PGF_{2\alpha}$ in HCTG hepatocytes (Supplementary Fig. 5). Collectively, these results indicated that FP promoted hepatic gluconeogenesis by enhancing gluconeogenic gene expression through CaMKIIγ/p38 signaling-mediated FOXO1 nuclear translocation.

Liver-Specific Deletion of FP Impairs Hepatic Gluconeogenesis in Mice

To exclude the effect of FP in other tissues on HGP, we created hepatocyte-specific FP-deficient mice using $FP^{F/F}$

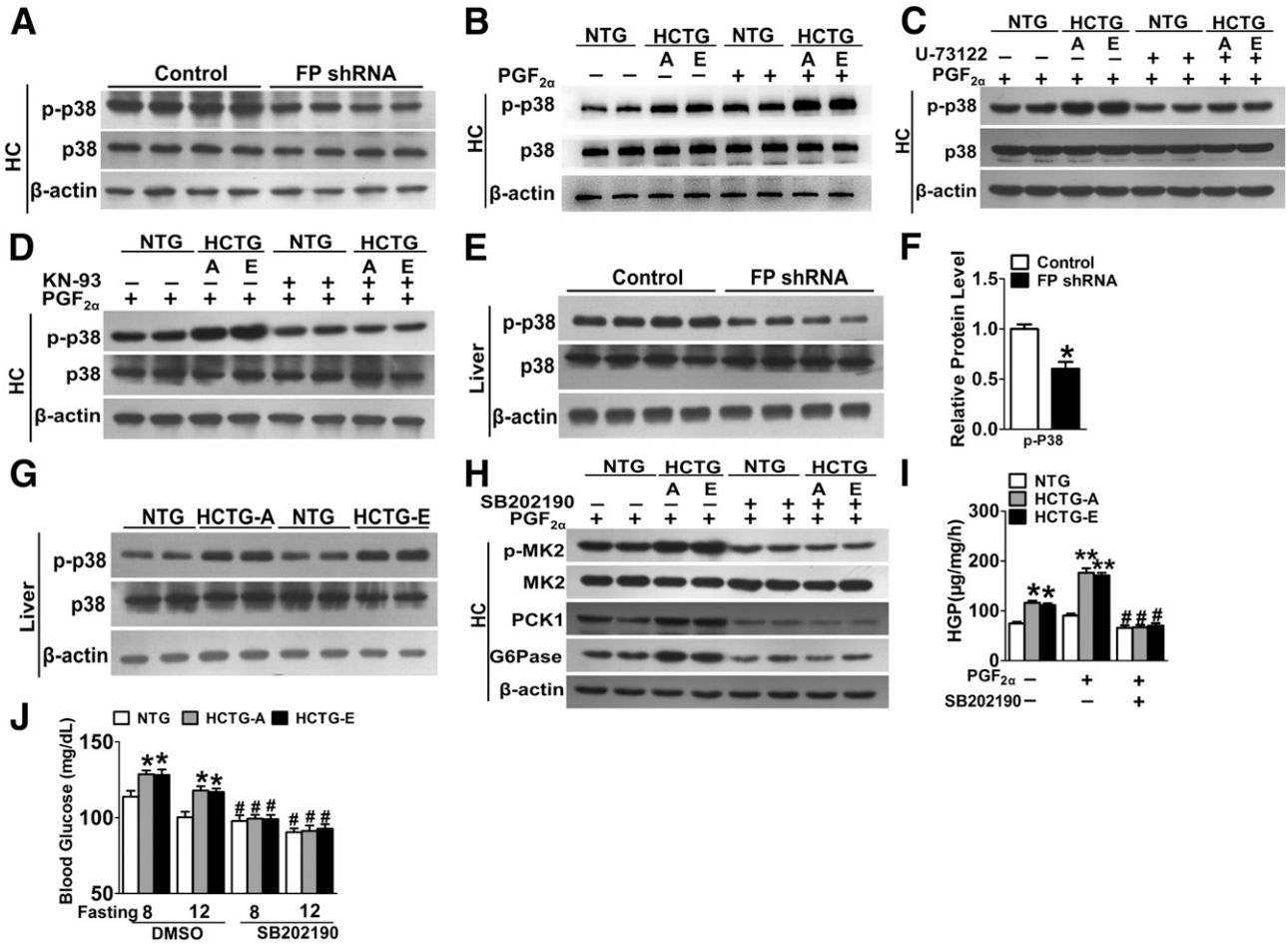

Figure 5—$PGF_{2\alpha}$ promotes hepatic gluconeogenesis by activating p38. *A*: Phosphorylated p38 (p-p38) levels in primary hepatocytes (HC) treated with FP shRNA or control adenovirus. *B*: Changes in p-p38 levels in NTG and HCTG hepatocytes in response to $PGF_{2\alpha}$ treatment. *C*: p-p38 levels in NTG and HCTG hepatocytes in the presence or absence of U73122 treatment. *D*: p-p38 levels in NTG and HCTG hepatocytes in the presence or absence of KN-93 treatment. *E*: Hepatic p-p38 levels in mice fasted for 8 h after infection with FP shRNA or control adenovirus. *F*: Quantification of p-p38 and total p38 expression in *E*. $^*P < 0.05$ vs. Control ($n = 8$). *G*: Hepatic p-p38 levels in NTG and HCTG mice after 8 h of fasting. *H*: PCK1, G6Pase, MK2, and p-MK2 protein levels in NTG and HCTG hepatocytes treated with the p38 inhibitor SB202190. *I*: Glucose production in NTG and HCTG hepatocytes treated with SB202190. $^*P < 0.05$ vs. NTG, $^{**}P < 0.01$ vs. NTG, $\#P < 0.05$ vs. with $PGF_{2\alpha}$ ($n = 4$). *J*: Blood glucose changes in NTG and HCTG mice upon fasting and in the presence or absence of SB202190 treatment. $^*P < 0.05$; $\#P < 0.05$ vs. DMSO ($n = 10$).

mice crossed with Alb^{cre} mice, which express Cre under the control of the albumin promoter (Supplementary Fig. 6*A* and *B*). This resulted in $FP^{F/F}Alb^{cre}$ mice in which the FP gene was specifically deleted in the liver (Supplementary Fig. 6*C*). $FP^{F/F}Alb^{cre}$ mice exhibited significantly lower blood glucose levels after 8–12 h of fasting (Fig. 7*A*), less HGP after pyruvate infusion (Fig. 7*B*), and increased sensitivity to insulin challenge compared with control mice (Fig. 7*C*). Moreover, hepatic deletion of FP significantly attenuated the phosphorylation of CaMKIIγ and p38, reduced nuclear translocation of FOXO1 without changing its total expression, and suppressed gluconeogenic gene expression (*G6pase* and *Pck1*) in the livers of $FP^{F/F}Alb^{cre}$ mice (Fig. 7*D*–*F*). These results showed that FP mediated hepatic gluconeogenesis via the CaMKIIγ/p38/FOXO1 signaling pathway (Fig. 7*H*).

FP Knockdown Improves Glucose Homeostasis in *ob/ob* Mice

Hepatic glucose output, such as that resulting from gluconeogenesis, is higher in subjects who are obese and have diabetes compared with that observed in subjects who are lean and do not have diabetes (31,32). To test whether silencing FP could improve glucose metabolism during obesity, *ob/ob* mice were infected with Ad-FP shRNA through tail-vein injection. As shown in Fig. 8*A*–*C*, hepatic knockdown of the FP receptor (Fig. 8*A*) significantly reduced blood glucose levels after 4-, 8-, and 12-h fasts (Fig. 8*B*), suppressed glucose production after PTT challenge (Fig. 8*C*), and improved insulin sensitivity in *ob/ob* mice (Fig. 8*D*). Accordingly, FP silencing also substantially inhibited the phosphorylation of CaMKIIγ and p38, impeded nuclear translocation of FOXO1, and suppressed gluconeogenic protein expression (G6pase and Pck1) in the livers of *ob/ob* mice (Fig. 8*E*–*G*).

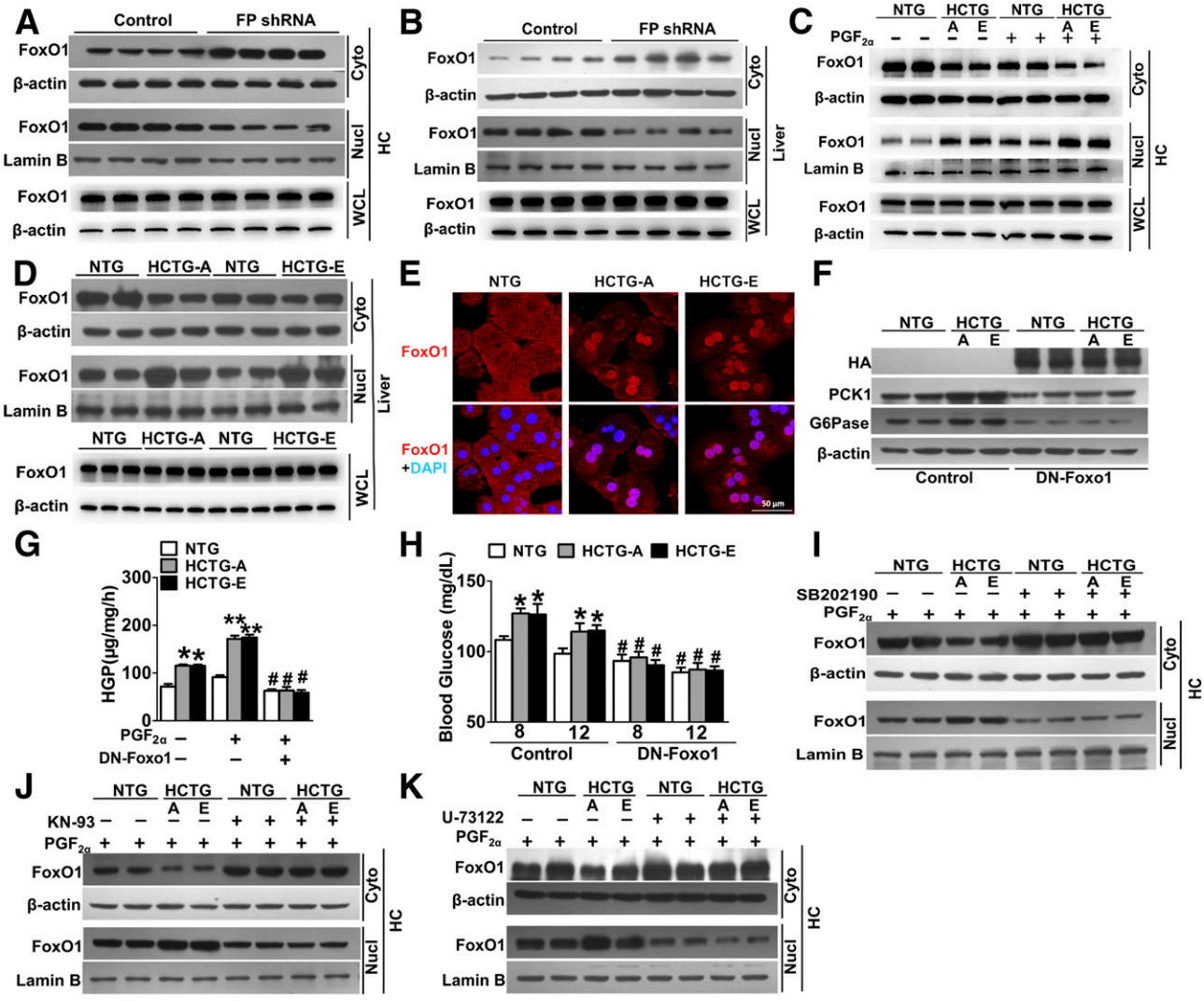

Figure 6—FP activation increases nuclear distribution of FOXO1 in the liver via the CaMKIIγ/p38 signaling pathway. *A*: Nuclear (Nucl), cytosolic (Cyto) distribution and whole cell lysate (WCL) of FOXO1 protein in primary hepatocytes (HC) infected with FP shRNA or control adenovirus. *B*: Hepatic nuclear and cytosolic distribution of FOXO1 protein in mice fasted for 8 h after FP shRNA or control adenovirus infusion. *C*: Nuclear and cytosolic distribution of FOXO1 protein in NTG and HCTG hepatocytes after $PGF_{2\alpha}$ challenge. *D*: Hepatic nuclear and cytosolic distribution of FOXO1 protein in NTG and HCTG mice fasted for 8 h. *E*: Immunofluorescence staining of FOXO1 in NTG and HCTG hepatocytes after $PGF_{2\alpha}$ treatment. *F*: PCK1, G6Pase, and HA-DN-FOXO1 protein levels in NTG and HCTG hepatocytes infected with DN-FOXO1 or control adenovirus. *G*: HGP in NTG and HCTG hepatocytes after infection with DN-FOXO1 adenovirus. $^{*}P < 0.05$ vs. NTG, $^{**}P < 0.01$ vs. NTG, #$P < 0.05$ vs. with $PGF_{2\alpha}$ ($n = 5$). *H*: Blood glucose levels in NTG and HCTG mice after 8 and 12 h of fasting and after DN-FOXO1 adenovirus infection. $^{*}P < 0.05$ vs. NTG, #$P < 0.05$ vs. DMSO ($n = 8$). *I–K*: Nuclear and cytosolic distribution of FOXO1 protein in NTG and HCTG hepatocytes treated with SB202190, KN-93, or U73122.

DISCUSSION

In obesity and type 2 diabetes, circulating levels of $PGF_{2\alpha}$ are markedly elevated (11), but the role of $PGF_{2\alpha}$ in glucose metabolism remains unknown. Here, we observed that the FP receptor was upregulated in the livers of fasting and obese mice and that hepatic FP deletion in hepatocytes suppressed HGP by downregulating the expression of gluconeogenic genes, whereas hFP overexpression in hepatocytes had an opposite effect. Mechanistically, FP activation enhanced the nuclear localization of FOXO1 and gluconeogenic gene translation through the Ca^{2+}/CaMKIIγ/p38 signaling pathway. These observations indicated that the FP-mediated gluconeogenic pathway might represent a potential therapeutic target for type 2 diabetes.

$PGF_{2\alpha}$ is a potent luteolytic agent that is also involved in modulating intraocular pressure and smooth muscle contraction in the uterus (11), with $PGF_{2\alpha}$ analogs, such as latanoprost, used in medicine to treat glaucoma (33). However, exaggerated $PGF_{2\alpha}$ production has been observed in patients experiencing rheumatic diseases (34), essential hypertension (35), obesity (36), and diabetes (37). Furthermore, FP deficiency reduces blood pressure and retards attendant atherogenesis in hyperlipidemic mice

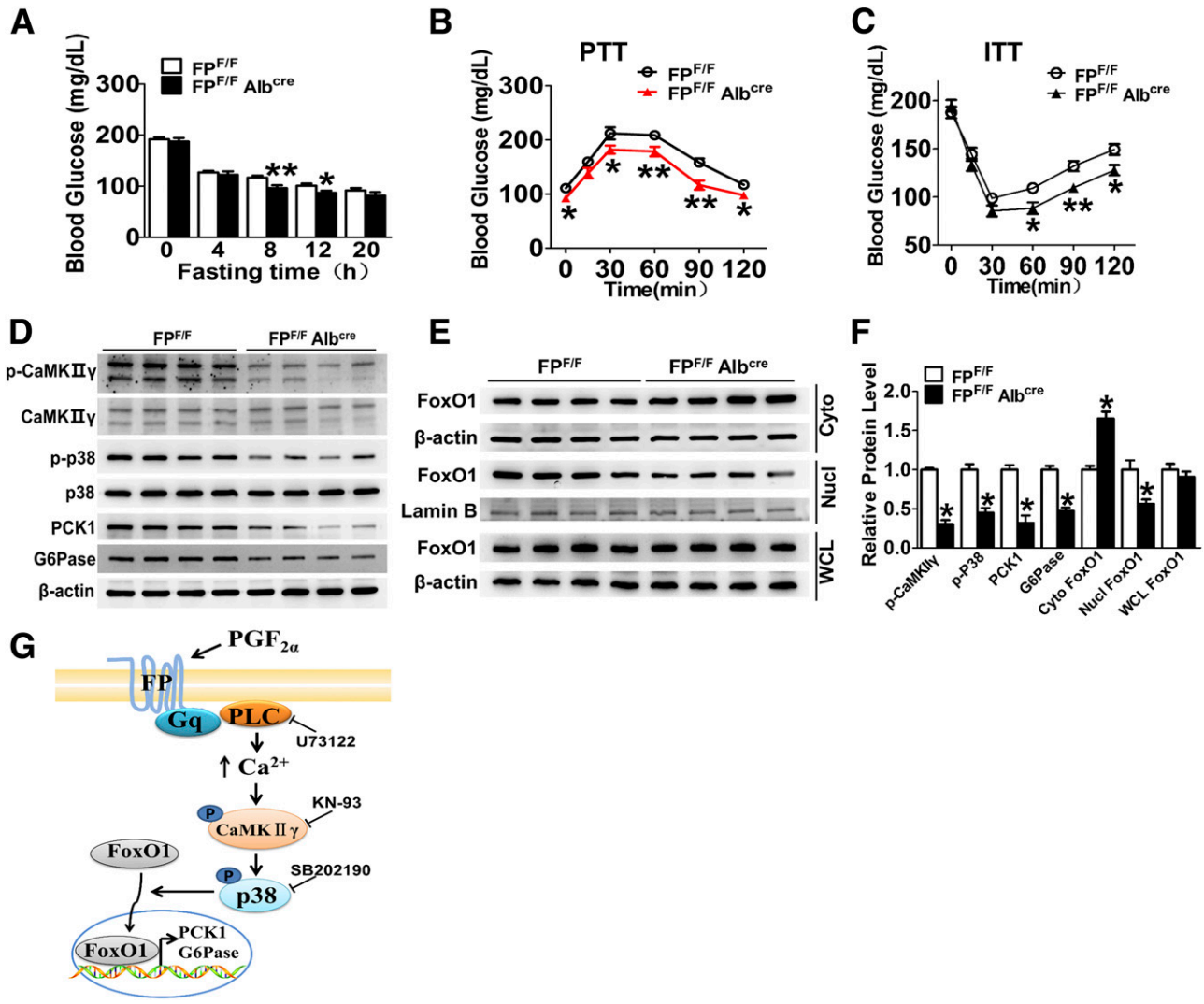

Figure 7—FP deficiency in hepatocytes impairs hepatic glucose output in mice after fasting. *A*: Plasma blood glucose levels in $FP^{F/F}$ and $FP^{F/F}Alb^{cre}$ mice after fasting for the indicated times. *$P < 0.05$; **$P < 0.01$ vs. $FP^{F/F}$ ($n = 10$). *B*: Blood glucose alterations in $FP^{F/F}$ and $FP^{F/F}Alb^{cre}$ mice according to PTT (2.0 g/kg pyruvate i.p.). *$P < 0.05$; **$P < 0.01$ vs. $FP^{F/F}$ ($n = 10$). *C*: Insulin tolerance test (ITT) in $FP^{F/F}Alb^{cre}$ and $FP^{F/F}$ mice. *$P < 0.05$; **$P < 0.01$ vs. $FP^{F/F}$ ($n = 10$). *D*: Hepatic phosphorylated CaMKIIγ (p-CaMKIIγ), CaMKIIγ, phosphorylated p38 (p-p38), p38, PCK1, and G6Pase protein levels in $FP^{F/F}$ and $FP^{F/F}Alb^{cre}$ mice after fasting for 8 h. *E*: Immunoblotting analysis of hepatic nuclear and cytosolic FOXO1 protein in $FP^{F/F}$ and $FP^{F/F}Alb^{cre}$ mice after fasting for 8 h. *F*: Quantification of p-CaMKIIγ, CaMKIIγ, p-p38, p38, PCK1, G6Pase expression, and FOXO1 distribution in cytoplasma (Cyto) and nuclear (Nucl) in *D* and *E*. *$P < 0.05$ vs. $FP^{F/F}$ ($n = 4$). *G*: Schematic diagram of FP-mediated hepatic gluconeogenesis through the G_q/CaMKIIγ/p38/FOXO1 signaling pathway. WCL, whole cell lysate.

(9). Interestingly, in this study, we observed that hepatic FP deletion markedly suppressed gluconeogenesis, whereas hepatic overexpression of hFP promoted gluconeogenesis in mice. In vitro, $PGF_{2\alpha}$ infusion directly stimulates hepatic glucose output in isolated rat livers (38). By contrast, endotoxin treatment attenuates hepatic gluconeogenesis in rats by downregulating expression of the FP receptor (39). Here, we found that FP silencing significantly improved insulin sensitivity in *ob/ob* mice, probably because of suppression of hepatic gluconeogenesis. Indeed, aspirin administration, which reduces PG production by inhibiting cyclooxygenase activity, dramatically reduces fasting plasma glucose in patients with type 2 diabetes and diabetic rats (40,41). Taken together, increased $PGF_{2\alpha}$ biosynthesis might lead to increased fasting or postprandial glucose levels in patients with type 2 diabetes.

In mammals, gluconeogenesis occurs mainly in the liver (42). FP receptor promotes G_q/Ca^{2+} signaling in hepatocytes and plays an important role in metabolism (43). In preadipocytes, $PGF_{2\alpha}$ binds G_q to modulate adipocyte differentiation by modulating intracellular Ca^{2+} signaling (44). Luteal regression in mammals mediated by $PGF_{2\alpha}$ also relies upon Ca^{2+}-dependent mechanism (45), suggesting the pivotal role of Ca^{2+} signaling in FP-mediated biological functions. Here, we found that FP receptor activated Ca^{2+}-dependent CaMKIIγ isoforms in hepatocytes and that

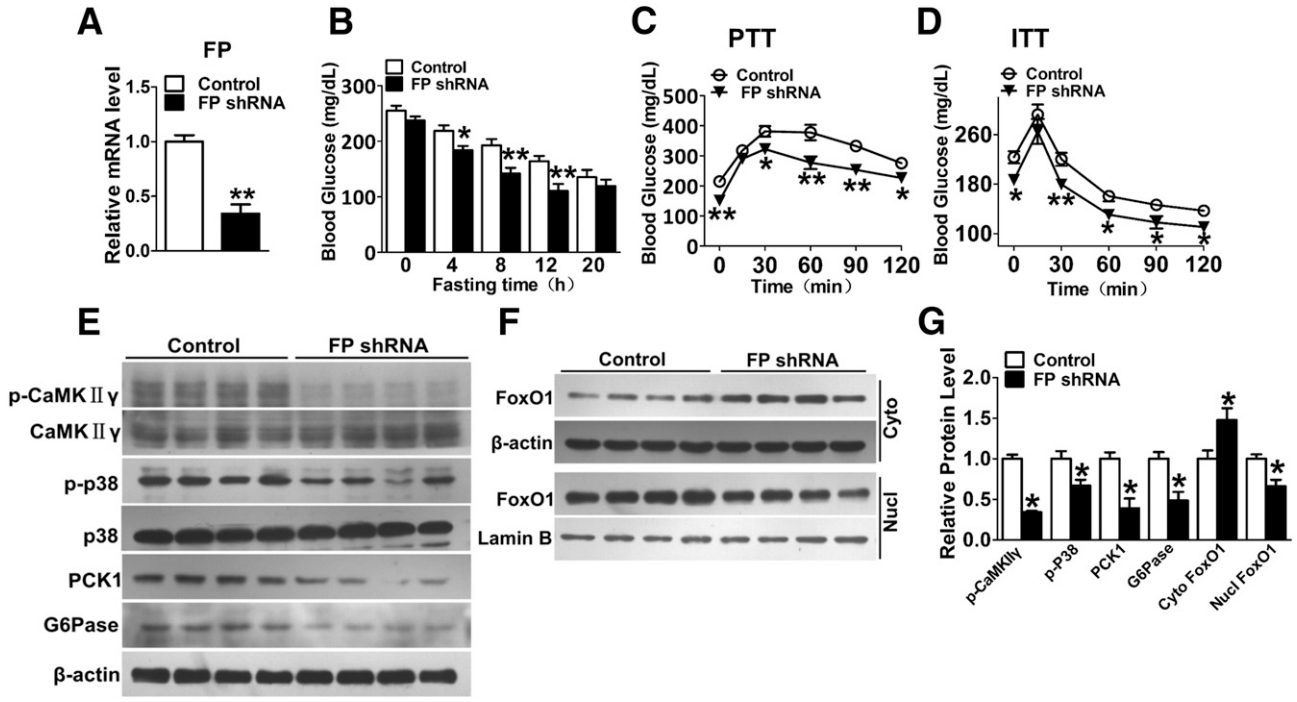

Figure 8—Knockdown of FP receptor improves glucose homeostasis in *ob/ob* mice. *A*: Hepatic FP expression in *ob/ob* mice after FP shRNA adenovirus infection. $^{**}P < 0.01$ vs. Control ($n = 8$). *B*: Plasma blood glucose levels in *ob/ob* mice after FP shRNA adenovirus infection. $^{*}P < 0.05$; $^{**}P < 0.01$ vs. Control ($n = 8$). *C*: Blood glucose alterations in *ob/ob* mice according to PTT (2.0 g/kg pyruvate i.p.) after FP shRNA adenovirus infection. $^{*}P < 0.05$; $^{**}P < 0.01$ vs. Control ($n = 8$). *D*: Insulin tolerance test (ITT) in *ob/ob* mice after FP shRNA adenovirus infection. $^{*}P < 0.05$; $^{**}P < 0.01$ vs. Control ($n = 8$). *E*: Hepatic phosphorylated CaMKIIγ (p-CaMKIIγ), CaMKIIγ, phosphorylated p38 (p-p38), p38, PCK1, and G6Pase protein levels in fasted *ob/ob* mice after FP shRNA adenovirus infection. *F*: Hepatic nuclear and cytosolic FOXO1 protein levels in fasted *ob/ob* mice after FP shRNA adenovirus infection. *G*: Quantification of p-CaMKIIγ, CaMKIIγ, p-p38, p38, PCK1, G6Pase expression, and FOXO1 distribution in cytoplasma (Cyto) and nuclear (Nucl) in *E* and *F*. $^{*}P < 0.05$ vs. Control ($n = 4$).

the inhibition of CaMKIIγ abrogated $PGF_{2\alpha}$-induced HGP. Notably, FP promoted gluconeogenic gene expression particularly through enhancing nuclear translocation of FOXO1 without influencing glycogenolytic gene expression. Indeed, Ca^{2+}/CaMKIIγ signaling promotes glucose production by promoting FOXO1 nuclear translocation in hepatocytes (26). Interestingly, we and others observed that genetic deficiency or inhibition of CaMKIIγ significantly decreases fasting-induced gluconeogenesis (26), suggesting that CaMKIIγ maybe serve as a potential therapeutic target for hyperglycemia and type 2 diabetes. Additionally, p38 is involved in the mediation of CaMKIIγ-driven FOXO1 nuclear translocation (26,27) and regulation of hepatic gluconeogenesis (28,46). In this study, we demonstrated that FP activation promoted p38 activity in livers and that p38 inhibition suppressed FP-mediated hepatic gluconeogenesis by reducing FOXO1 nuclear translocation. In agreement with our findings, p38 is a key signaling molecule involved in various FP-mediated physiological functions, such as myometrial contractility during gestation (47), corpus luteum regression (48), cardiomyocyte hypertrophy (49), and artery contraction (50). Therefore, our findings suggest that FP promotes hepatic gluconeogenesis by activating the CaMKIIγ/p38/FOXO1 signaling pathway.

In summary, we demonstrated that the $PGF_{2\alpha}$/FP axis facilitates hepatic gluconeogenesis during fasting and obesity through CaMKIIγ/p38 signaling, suggesting that targeting the $PGF_{2\alpha}$/FP signaling pathway might represent a promising therapeutic strategy for treating type 2 diabetes.

Acknowledgments. The authors thank Dr. Akiyoshi Fukamizu (University of Tsukuba, Tsukuba, Japan) for providing WT-FLAG-FOXO1 and 9A-FIAG-FOXO1 plasmids.

Funding. This work was supported by the National Natural Science Foundation of China (81525004, 91439204, 91639302, 31771269, and 31200860) and the National Key R&D Program from the Ministry of Science and Technology of China (2017YFC1307404 and 2017YFC1307402). Yi.Y. is a Fellow at the Jiangsu Collaborative Innovation Center for Cardiovascular Disease Translational Medicine.

Duality of Interest. No potential conflicts of interest relevant to this article were reported.

Author Contributions. Y.W. acquired the data, performed statistical analysis, and drafted the manuscript. S.Y., B.X., S.Z., Q.Z., G.C., Q.L., Y.L., Yu Y., and D.C. acquired the data. Yi.Y. handled funding and supervision. Yi.Y. and Y.S. conceived and designed the research. Yi.Y. and Y.S. made critical revision of the manuscript for key intellectual content. Yi.Y. is the guarantor of this work and, as such, had full access to all the data in the study and takes responsibility for the integrity of the data and the accuracy of the data analysis.

References

1. Chatterjee S, Khunti K, Davies MJ. Type 2 diabetes. Lancet 2017;389:2239–2251
2. Goldfine AB, Shoelson SE. Therapeutic approaches targeting inflammation for diabetes and associated cardiovascular risk. J Clin Invest 2017;127:83–93
3. Rines AK, Sharabi K, Tavares CD, Puigserver P. Targeting hepatic glucose metabolism in the treatment of type 2 diabetes. Nat Rev Drug Discov 2016;15:786–804
4. Wang Y, Viscarra J, Kim SJ, Sul HS. Transcriptional regulation of hepatic lipogenesis. Nat Rev Mol Cell Biol 2015;16:678–689
5. Wunderlich FT, Ströhle P, Könner AC, et al. Interleukin-6 signaling in liver-parenchymal cells suppresses hepatic inflammation and improves systemic insulin action. Cell Metab 2010;12:237–249
6. Staehr P, Hother-Nielsen O, Landau BR, Chandramouli V, Holst JJ, Beck-Nielsen H. Effects of free fatty acids per se on glucose production, gluconeogenesis, and glycogenolysis. Diabetes 2003;52:260–267
7. Yan S, Zhang Q, Zhong X, et al. I prostanoid receptor-mediated inflammatory pathway promotes hepatic gluconeogenesis through activation of PKA and inhibition of AKT. Diabetes 2014;63:2911–2923
8. Kim SO, Markosyan N, Pepe GJ, Duffy DM. Estrogen promotes luteolysis by redistributing prostaglandin F2α receptors within primate luteal cells. Reproduction 2015;149:453–464
9. Yu Y, Lucitt MB, Stubbe J, et al. Prostaglandin F2alpha elevates blood pressure and promotes atherosclerosis. Proc Natl Acad Sci U S A 2009;106:7985–7990
10. Agas D, Marchetti L, Hurley MM, Sabbieti MG. Prostaglandin F2α: a bone remodeling mediator. J Cell Physiol 2013;228:25–29
11. Zhang J, Gong Y, Yu Y. PG F(2α) receptor: a promising therapeutic target for cardiovascular disease. Front Pharmacol 2010;1:116
12. Basu S, Larsson A, Vessby J, Vessby B, Berne C. Type 1 diabetes is associated with increased cyclooxygenase- and cytokine-mediated inflammation. Diabetes Care 2005;28:1371–1375
13. Helmersson J, Vessby B, Larsson A, Basu S. Association of type 2 diabetes with cyclooxygenase-mediated inflammation and oxidative stress in an elderly population. Circulation 2004;109:1729–1734
14. Monnier L, Mas E, Ginet C, et al. Activation of oxidative stress by acute glucose fluctuations compared with sustained chronic hyperglycemia in patients with type 2 diabetes. JAMA 2006;295:1681–1687
15. Fennekohl A, Schieferdecker HL, Jungermann K, Püschel GP. Differential expression of prostanoid receptors in hepatocytes, Kupffer cells, sinusoidal endothelial cells and stellate cells of rat liver. J Hepatol 1999;30:38–47
16. Xiao B, Gu SM, Li MJ, et al. Rare SNP rs12731181 in the miR-590-3p target aite of the prostaglandin F2α receptor gene confers risk for essential hypertension in the Han Chinese population. Arterioscler Thromb Vasc Biol 2015;35:1687–1695
17. Ichinose K, Juang YT, Crispín JC, Kis-Toth K, Tsokos GC. Suppression of autoimmunity and organ pathology in lupus-prone mice upon inhibition of calcium/calmodulin-dependent protein kinase type IV. Arthritis Rheum 2011;63:523–529
18. O'Sullivan AW, Wang JH, Redmond HP. p38 MAP kinase inhibition promotes primary tumour growth via VEGF independent mechanism. World J Surg Oncol 2009;7:89
19. Luo J, Deng ZL, Luo X, et al. A protocol for rapid generation of recombinant adenoviruses using the AdEasy system. Nat Protoc 2007;2:1236–1247
20. Asada S, Daitoku H, Matsuzaki H, et al. Mitogen-activated protein kinases, Erk and p38, phosphorylate and regulate Foxo1. Cell Signal 2007;19:519–527
21. Yan S, Tang J, Zhang Y, et al. Prostaglandin E_2 promotes hepatic bile acid synthesis by an E prostanoid receptor 3-mediated hepatocyte nuclear receptor 4α/cholesterol 7α-hydroxylase pathway in mice. Hepatology 2017;65:999–1014
22. Stanya KJ, Jacobi D, Liu S, et al. Direct control of hepatic glucose production by interleukin-13 in mice. J Clin Invest 2013;123:261–271
23. Shen Y, Zuo S, Wang Y, et al. Thromboxane governs the differentiation of adipose-derived stromal cells toward endothelial cells in vitro and in vivo. Circ Res 2016;118:1194–1207
24. Liu Y, Dentin R, Chen D, et al. A fasting inducible switch modulates gluconeogenesis via activator/coactivator exchange. Nature 2008;456:269–273
25. Smyth EM, Grosser T, Wang M, Yu Y, FitzGerald GA. Prostanoids in health and disease. J Lipid Res 2009;50(Suppl.):S423–S428
26. Ozcan L, Wong CC, Li G, et al. Calcium signaling through CaMKII regulates hepatic glucose production in fasting and obesity. Cell Metab 2012;15:739–751
27. Ozcan L, Cristina de Souza J, Harari AA, Backs J, Olson EN, Tabas I. Activation of calcium/calmodulin-dependent protein kinase II in obesity mediates suppression of hepatic insulin signaling. Cell Metab 2013;18:803–815
28. Jing Y, Liu W, Cao H, et al. Hepatic p38α regulates gluconeogenesis by suppressing AMPK. J Hepatol 2015;62:1319–1327
29. Lee S, Dong HH. FoxO integration of insulin signaling with glucose and lipid metabolism. J Endocrinol 2017;233:R67–R79
30. Kitamura YI, Kitamura T, Kruse JP, et al. FoxO1 protects against pancreatic beta cell failure through NeuroD and MafA induction. Cell Metab 2005;2:153–163
31. Basu R, Chandramouli V, Dicke B, Landau B, Rizza R. Obesity and type 2 diabetes impair insulin-induced suppression of glycogenolysis as well as gluconeogenesis. Diabetes 2005;54:1942–1948
32. Gastaldelli A, Baldi S, Pettiti M, et al. Influence of obesity and type 2 diabetes on gluconeogenesis and glucose output in humans: a quantitative study. Diabetes 2000;49:1367–1373
33. Woodward DF, Wang JW, Poloso NJ. Recent progress in prostaglandin F2α ethanolamide (prostamide F2α) research and therapeutics. Pharmacol Rev 2013;65:1135–1147
34. Basu S, Whiteman M, Mattey DL, Halliwell B. Raised levels of F(2)-isoprostanes and prostaglandin F(2alpha) in different rheumatic diseases. Ann Rheum Dis 2001;60:627–631
35. Guarneri M, Geraci C, Incalcaterra F, et al. Subclinical atherosclerosis and fetuin-A plasma levels in essential hypertensive patients. Hypertens Res 2013;36:129–133
36. Sinaiko AR, Steinberger J, Moran A, et al. Relation of body mass index and insulin resistance to cardiovascular risk factors, inflammatory factors, and oxidative stress during adolescence. Circulation 2005;111:1985–1991
37. Davì G, Ciabattoni G, Consoli A, et al. In vivo formation of 8-iso-prostaglandin f2alpha and platelet activation in diabetes mellitus: effects of improved metabolic control and vitamin E supplementation. Circulation 1999;99:224–229
38. Spitzer JA, Deaciuc IV. Prostaglandin F2 alpha stimulates gluconeogenesis in the perfused rat liver and this effect is blunted in livers from endotoxin infused rats. Agents Actions 1990;31:341–344
39. Deaciuc IV, Spitzer JA. Down-regulation of prostaglandin F2 alpha receptors in rat liver during chronic endotoxemia. Prostaglandins Leukot Essent Fatty Acids 1991;42:191–195
40. Hundal RS, Petersen KF, Mayerson AB, et al. Mechanism by which high-dose aspirin improves glucose metabolism in type 2 diabetes. J Clin Invest 2002;109:1321–1326
41. Amiri L, John A, Shafarin J, et al. Enhanced glucose tolerance and pancreatic beta cell function by low dose aspirin in hyperglycemic insulin-resistant type 2 diabetic Goto-Kakizaki (GK) rats. Cell Physiol Biochem 2015;36:1939–1950
42. Han HS, Kang G, Kim JS, Choi BH, Koo SH. Regulation of glucose metabolism from a liver-centric perspective. Exp Mol Med 2016;48:e218
43. Koukoui O, Boucherie S, Sezan A, Prigent S, Combettes L. Effects of the prostaglandins PGF2alpha and PGE2 on calcium signaling in rat hepatocyte doublets. Am J Physiol Gastrointest Liver Physiol 2006;290:G66–G73
44. Liu L, Clipstone NA. Prostaglandin F2alpha inhibits adipocyte differentiation via a G alpha q-calcium-calcineurin-dependent signaling pathway. J Cell Biochem 2007;100:161–173
45. Stocco CO, Lau LF, Gibori G. A calcium/calmodulin-dependent activation of ERK1/2 mediates JunD phosphorylation and induction of nur77 and 20alpha-hsd genes by prostaglandin F2alpha in ovarian cells. J Biol Chem 2002;277:3293–3302

46. Cao W, Collins QF, Becker TC, et al. p38 Mitogen-activated protein kinase plays a stimulatory role in hepatic gluconeogenesis. J Biol Chem 2005;280: 42731–42737

47. Xu C, You X, Liu W, et al. Prostaglandin F2α regulates the expression of uterine activation proteins via multiple signalling pathways. Reproduction 2015;149:139–146

48. Zhang X, Li J, Liu J, Luo H, Gou K, Cui S. Prostaglandin F2α upregulates Slit/Robo expression in mouse corpus luteum during luteolysis. J Endocrinol 2013;218:299–310

49. Adams JW, Sah VP, Henderson SA, Brown JH. Tyrosine kinase and c-Jun NH2-terminal kinase mediate hypertrophic responses to prostaglandin F2alpha in cultured neonatal rat ventricular myocytes. Circ Res 1998;83:167–178

50. Knock GA, De Silva AS, Snetkov VA, et al. Modulation of PGF2alpha- and hypoxia-induced contraction of rat intrapulmonary artery by p38 MAPK inhibition: a nitric oxide-dependent mechanism. Am J Physiol Lung Cell Mol Physiol 2005; 289:L1039–L1048